

Fuel Cell Reformer Control Design

May 8, 2006

Karel Schnebele

Abstract:

Fuel cells are a viable low polluting and sustainable alternative energy source. They require a reformer to convert a fuel source, like methane, to hydrogen for operation. The purpose of this report is to develop a final project for a control class. This report explains how a system differential of equations modeling pertinent steam reformer temperatures was converted to a linear state space model that can be manipulated in Simulink for the development of a control strategy. This report develops a multivariable IMC-based PID controller to provide quick response to setpoint changes and disturbances for a steam reformer. It outlines the SISO controller development and uses a relative gain array analysis to correctly pair the multivariable control loops. The multivariable control strategy was then subjected to an SVD analysis to determine the directional sensitivity of the system. This control system is adequate in setpoint tracking and disturbance rejection but the system itself has a limited range of directions it can move in.

Section 1: Background

Fuel cells are important emerging technologies that can convert fuels to electricity without generating any pollution when hydrogen is used as the fuel source (Radulescu et al., 2006). One of the many issues involved in fuel cell operation is maintaining a constant supply of hydrogen ions to the stack as a source of fuel. Fuel cell reformers turn a source of fuel, like methane, petroleum, or biofuels, into hydrogen ions. There are a number of different methods of reforming these base fuels into hydrogen, but one of the more mature methods that is widely practiced in industry is steam reforming (Larminie and Dicks, 2003).

Since hydrogen is not a readily available or distributable fuel source, steam reformers can use natural gas as their base fuel to create hydrogen for the fuel cell. The main variables affecting the effectiveness of hydrogen production in the reformer are the excess air ratio and the reformer catalyst bed temperature (Pukrushpan et al., 2005). The temperature at the outlet of the reformer is determined by the excess air ratio which specifies how much air beyond that stoichiometrically required for the oxidation of methane is supplied to the reformer. The outlet temperature must fall between a low temperature that will cause soot formation and the maximum operating temperature of the fuel cell (Meshcheryakov et al., 2005). For an application like a domestic micro-CHP (Combined Heat and Power) the highest concentration of hydrogen gas is produced at a temperature of 650 deg C where the heat to the reformer is provided by a burner (Radulescu et al., 2006).

Steam reforming can also be accomplished inside the fuel cell stack to take advantage of the heat generated by the stack to provide the necessary temperatures for the conversion of methane to hydrogen. In indirect internal reforming the reformer is placed in close proximity to the stack and receives its heat from operation of the fuel cell. In direct internal reforming the high temperature of a solid oxide fuel cell provides enough heat to allow the reforming reactions to occur directly in the anode (Dicks, 1998). In a direct internal reforming system the endothermic reforming reactions can help offset the exothermic reactions of the fuel cell. Temperature control is still necessary because in a .78 V fuel cell the heat produced in the stack is almost double the amount of heat

consumed in the reforming process, but the internal system significantly decreases the amount of air needed for cooling (Dicks, 1998).

In a partial oxidation reformer the main goals of the control system are to provide enough hydrogen gas to supply the fuel cell, maintain the temperature of the catalytic partial oxidation reformer, and ensure the efficiency of the entire system (Pukrushpan et al 2005). These goals are similar to the control objectives in a steam reforming system. The control of a partial oxidation reformer is too complex to model with a decentralized controller. Multivariable control is more effective and a linear quadratic method can be used to design controllers (Pukrushpan et al, 2005).

Section 2: Steam Reformer Model Development

This report is based off the steam reformer model developed by Jahn and Schroer (2005). That paper develops a dynamic simulation of a steam reformer in a 40 cell proton exchange membrane (PEM) residential fuel cell plant with a nominal power of 5kW. The reformer operates at temperatures around or above 500 deg C and has a methane flow rate between 10 and 25 standard liters per minute (SLPM) to the burner. The water flow rate is given by the steam to carbon molar ratio which is approximately 3.5. In the paper the reformer generates reformatate at a rate of either 40 or 70 SLPM and operates at a pressure of 3.5 bars. A process and instrumentation diagram is given in Figure 1. The dynamic equations developed in the paper are given below.

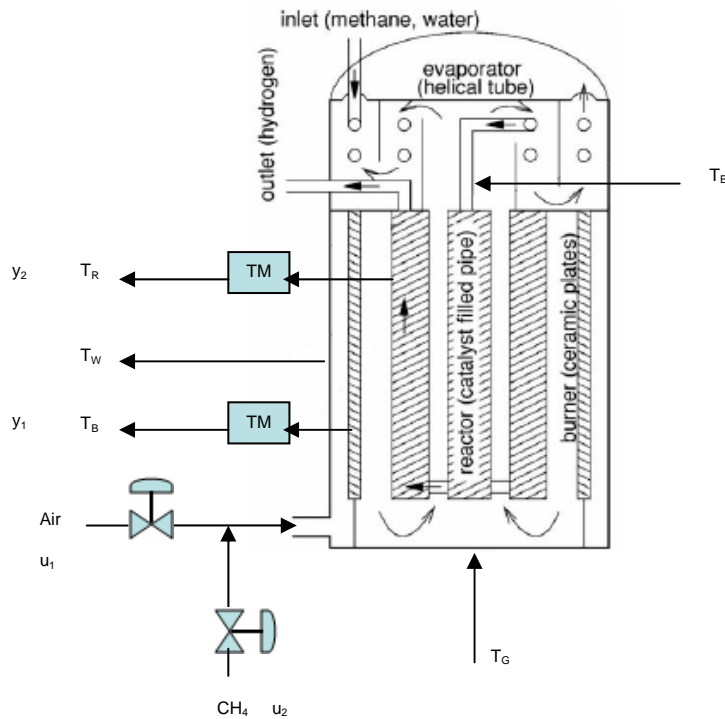


Figure 1: The steam reformer process and instrumentation diagram. Image adapted from Jahn and Schroer (2005).

$$f_1: C_W \frac{dT_W}{dt} = k_{GW}(T_G - T_W) - k_{WA}(T_W - T_A) - c_{p,B} \cdot \dot{n}_B (T_W - T_A) \quad [1]$$

$$f_2: C_G \frac{dT_G}{dt} = k_{BG}(T_B - T_G) - k_{GW}(T_G - T_W) + k_{FG} \cdot c_{p,F} \cdot \dot{n}_F (T_F - T_G) \quad [2]$$

$$f_3: C_B \frac{dT_B}{dt} = k_{FB}(T_F - T_B) - c_{p,B} \cdot \dot{n}_B (T_B - T_W) - k_{BR}(T_B^4 - T_R^4) - k_{BG}(T_B - T_G) \quad [3]$$

$$f_4: C_E \frac{dT_E}{dt} = k_{RE}(T_R - T_E) + c_{p,F} \cdot \dot{n}_F (T_R - T_E) - r \cdot \dot{n}_{H_2O,i} - c_{p,H_2O} \cdot \dot{n}_{H_2O} (T_E - T_{H_2O}) - c_{p,CH_4} \cdot \dot{n}_{CH_4} (T_E - T_{CH_4}) - k_{EA}(T_E - T_A) \quad [4]$$

$$f_5: C_R \frac{dT_R}{dt} = k_{BR}(T_B^4 - T_R^4) - k_{RE}(T_R - T_E) + c_{p,F} \cdot \dot{n}_F (T_{FG} - T_R) - \Delta h_0 \cdot \Delta \dot{n}_0 - \Delta h_1 \cdot \Delta \dot{n}_1 - c_{p,H_2O} \cdot \dot{n}_{H_2O} (T_R - T_E) - c_{p,CH_4} \cdot \dot{n}_{CH_4} (T_R - T_E) \quad [5]$$

T_W is the wall temperature, T_G is the temperature of the ground plate, T_B is the burner temperature, T_E is the evaporator temperature, T_R is the reformer temperature, T_A is the ambient air temperature, and T_{FG} is the flue gas temperature. The \dot{n} terms indicate molar flow rates, c_p terms are specific heats, k terms are heat exchange coefficients which are constant in this system, Δh values are heats of reaction given in the paper, and Δn values are the extent of the reaction which is a function of the reformer temperature and steam to carbon ratio. Figure 2 is the model structure from the paper which shows how the different components are related. Table 1 is the table from the paper that defines the constants for the system and Table 2 is from the paper and defines the equations for the burner and flue gas flow rates where \dot{n}_v is the methane flow rate to the burner and λ is the excess air ratio to the burner. The burner and flue gas flow rates were determined assuming the burner was on.

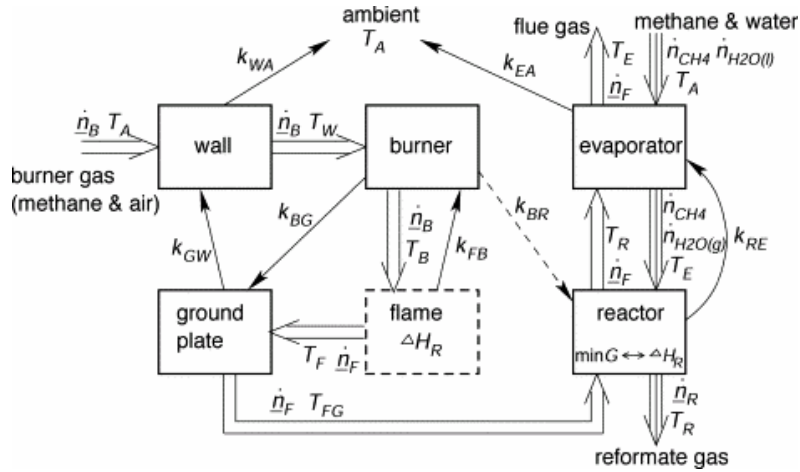


Figure 2: The boxes correspond to the lumped elements, single lines depict heat transfer (solid is conduction, dashed is radiation), double lines depict the burner gas flow, and triple lines depict the reformat gas flow. Image from Jahn and Schroer (2005).

Table 1

Model parameters

Parameter	Identified Value	Unit
C_W	7.27×10^3	J/K
C_B	0.22×10^3	J/K
C_E	5.42×10^3	J/K
C_G	2.44×10^3	J/K
C_R	3.61×10^3	J/K
v_0	-2.46×10^{-4}	mol/s
v_1	4.10×10^{-3}	mol V/s
k_{BR}	1.32×10^{-9}	W/K ⁴
k_{BG}	4.50	W/K
k_{GW}	5.16	W/K
k_{EA}	0.439	W/K
k_{RE}	16.3	W/K
k_{WA}	1.16	W/K
k_{FB}	16.1	W/K
k_{FG}	0.30	–

Table 2

Burner and flue gas flow rates depending on the burner state

Component	Fan on	Burner on
\dot{n}_{B,O_2}	$2\lambda\dot{n}_V$	$2\lambda\dot{n}_V$
\dot{n}_{B,N_2}	$2\frac{79}{21}\lambda\dot{n}_V$	$2\frac{79}{21}\lambda\dot{n}_V$
\dot{n}_{B,CH_4}	0	\dot{n}_V
\dot{n}_{F,O_2}	$2\lambda\dot{n}_V$	$2(\lambda - 1)\dot{n}_V$
\dot{n}_{F,N_2}	$2\frac{79}{21}\lambda\dot{n}_V$	$2\frac{79}{21}\lambda\dot{n}_V$
\dot{n}_{F,CO_2}	0	\dot{n}_V
\dot{n}_{F,H_2O}	0	$2\dot{n}_V$

The specific heats are temperature dependent variables with the following correlations.

$$c_p = R(A + B(T) + C(T^2) + D(T^{-2})) \quad [6]$$

A, B, C, and D are all heat capacity coefficients that depend on the compound, R is the gas constant, and T is temperature. The total burner and flue gas flow rates were determined by adding the flow rates of each component gas. After defining the heat capacities and individual flow rates for each gas the heat capacity of the burner and flue gas were determined by a weighted average procedure. The total heat capacity is the sum of each individual heat capacity multiplied by its fraction of the total flow.

All these correlations and equations were put into an m-file in Matlab, available in Appendix 1.2, where the variables were the steam to carbon ratio, the excess air value, and the initial methane flow rate to the reformer. Figures 3 through 8 show the affect of changing the variables on the steady state temperatures where the temperature on the graphs are in deg C. A difference in the initial methane flow rate to the reformer of 5 SLPM causes a reformer temperature difference of 144 deg C and a burner temperature difference of 90 deg C. A difference in the steam to carbon ratio of 1 causes a reformer temperature difference of 98 deg C and a burner temperature difference of 53 deg C. A difference in the excess air ratio of 1 causes a reformer temperature difference of 153 deg C and a burner temperature difference of 179 deg C.

Affect of changing the initial methane flow rate to the reformer

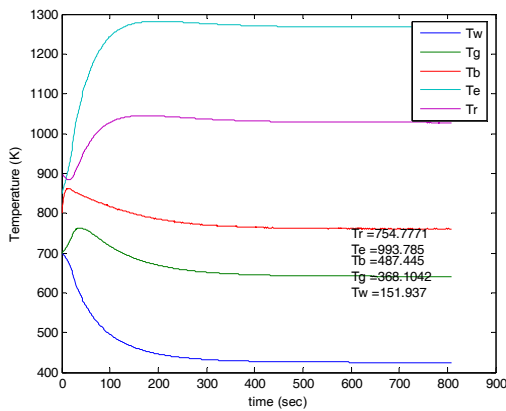


Figure 3: Output temperatures with an initial methane flow rate of 10 SLM, a steam to carbon ratio of 3.5, and an excess air ratio of 5.

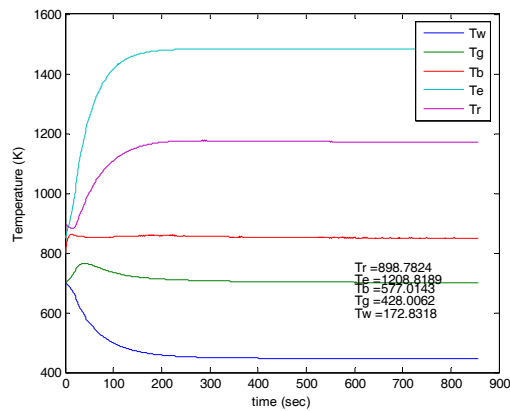


Figure 4: Output temperatures with an initial methane flow rate of 15 SLM, a steam to carbon ratio of 3.5, and an excess air ratio of 5.

Affect of changing the steam to carbon ratio to the reformer

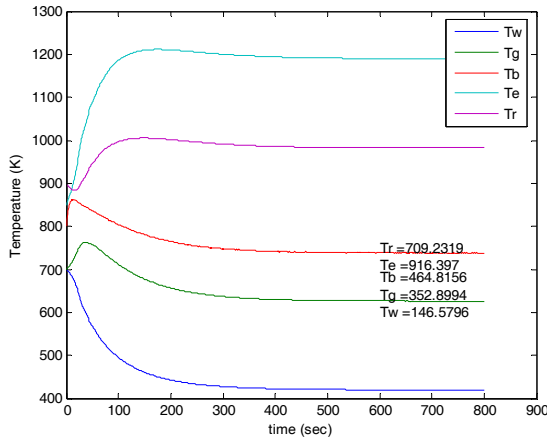


Figure 5: Output temperatures with an initial methane flow rate of 10 SLPM, a steam to carbon ratio of 3, and an excess air ratio of 5.

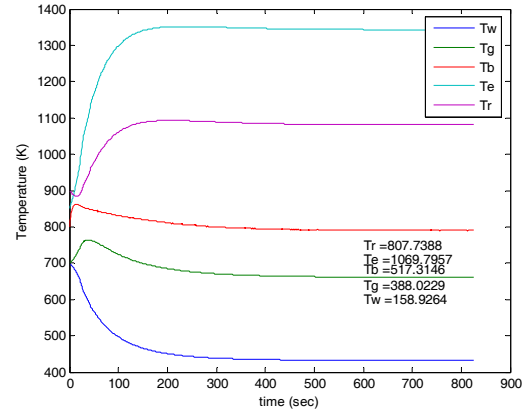


Figure 6: Output temperatures with an initial methane flow rate of 10 SLPM, a steam to carbon ratio of 4, and an excess air ratio of 5.

Affect of changing the excess air ratio to the burner

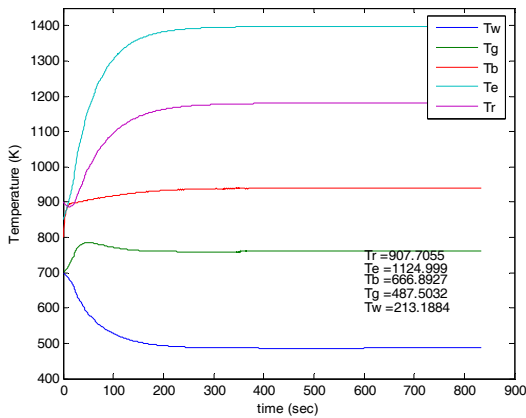


Figure 7: Output temperatures with an initial methane flow rate of 10 SLPM, a steam to carbon ratio of 3.5, and an excess air ratio of 4.

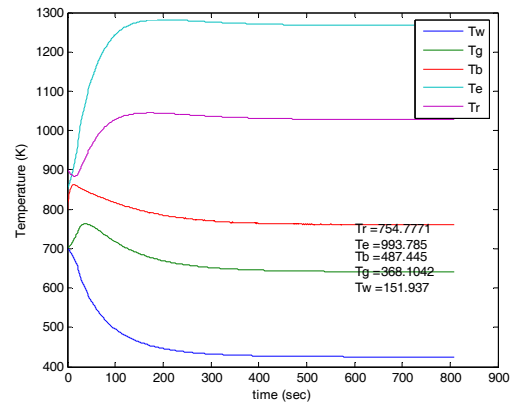


Figure 8: Output temperatures with an initial methane flow rate of 10 SLPM, a steam to carbon ratio of 3.5, and an excess air ratio of 5.

To create a state space model the equations needed to be linearized around specified values. The reformer needs to operate around a temperature of 700 deg C, the steam to carbon ratio should be around 3, and the methane flow rate should be around 10 SLPM for a mid-level power setting. After a number of iterations to obtain a reformer temperature of 700 deg C, the methane flow rate is 9.5 SLPM, the steam to carbon ratio is 3.0076, and the excess air ratio is 5. Figure 9 shows the output temperatures under these defined conditions where the steady state wall plate temperature is 145.5671 deg C, the

steady state ground plate temperature is 350.0323 deg C, the steady state burner temperature is 460.524 deg C, the steady state evaporator temperature is 897.0203 deg C, and the steady state reformer temperature is 700.003 deg C.

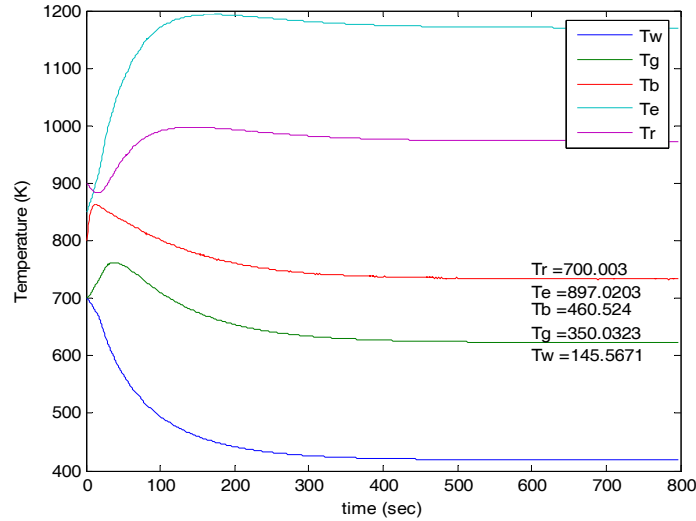


Figure 9: Output temperatures with the steam to carbon ratio, excess air ratio, and initial methane flow rate to the reformer defined.

These differential equations must be converted into a state space model before a control strategy can be developed. In the model the functions were given in equations 1 through 5, the states are the deviations in the output temperatures, the inputs are the excess air ratio and the methane flow rate to the burner, and the outputs are the burner and reformer temperatures. The reformer temperature is an output because the temperature directly affects the creation of the hydrogen fuel source. The burner temperature was chosen as the other output because the burner provides the heat source for the endothermic reforming reaction. The methane flow rate to the burner was chosen as an input because it is a variable feedstream to the burner and the excess air ratio was chosen because it is a natural input variable. The nominal value of the methane flow rate, determined by the steady state temperature values defined above, is 6.5856 SLPM. Below are the states, inputs, and outputs in deviation variable form.

$$\text{States} = \begin{bmatrix} x_1 \\ x_2 \\ x_3 \\ x_4 \\ x_5 \end{bmatrix} = \begin{bmatrix} T_W - T_{Ws} \\ T_G - T_{Gs} \\ T_B - T_{Bs} \\ T_E - T_{Es} \\ T_R - T_{Rs} \end{bmatrix} \quad [7]$$

$$\text{Inputs} = \begin{bmatrix} u_1 \\ u_2 \end{bmatrix} = \begin{bmatrix} \text{excess air ratio } (\lambda) \\ nv \end{bmatrix} \quad [8]$$

$$\text{Outputs} = \begin{bmatrix} g_1 \\ g_2 \end{bmatrix} = \begin{bmatrix} y_1 \\ y_2 \end{bmatrix} = \begin{bmatrix} T_B \\ T_R \end{bmatrix} \quad [9]$$

The linear state space form is

$$\begin{aligned} \dot{x}' &= Ax' + Bu' \\ y' &= Cx' + Du' \end{aligned} \quad [10]$$

and elements of the matrices are as follow

$$A_{ij} = \frac{\partial f_i}{\partial x_j} \quad B_{ij} = \frac{\partial f_i}{\partial u_j} \quad C_{ij} = \frac{\partial g_i}{\partial x_j} \quad D_{ij} = \frac{\partial g_i}{\partial u_j} \quad [11]$$

where the subscript ij corresponds to the ith row and the jth column of the matrix. The sample calculations for the matrices are given in Appendix 1.2. The final A, B, C, and D matrices are given below.

$$A = \begin{bmatrix} -0.001593 & 7.098 \times 10^{-4} & 0 & 0 & 0 \\ 0.002115 & -0.004911 & 0.0018443 & 0 & 0 \\ 0.034462 & 0.020455 & -0.058625 & 0 & -0.008232 \\ 0 & 0 & 0 & -0.00472 & 0.004436 \\ 0 & 0 & 1.4285 \times 10^{-4} & 0.004675 & -0.007322 \end{bmatrix} \quad [12]$$

$$B = \begin{bmatrix} -0.02424 & -25.888 \\ 0.14687 & 156.0762 \\ -2.0898 & -2032.8766 \\ -0.05429 & -57.6894 \\ -0.075294 & -80.0119 \end{bmatrix} \quad [13]$$

$$C = \begin{bmatrix} 0 & 0 & 1 & 0 & 0 \\ 0 & 0 & 0 & 0 & 1 \end{bmatrix} \quad D = \begin{bmatrix} 0 & 0 \\ 0 & 0 \end{bmatrix} \quad [14]$$

These matrices were used to develop a Simulink subsystem on which a variety of control strategies could be implemented. The Simulink block diagram is given below in Figure 10.

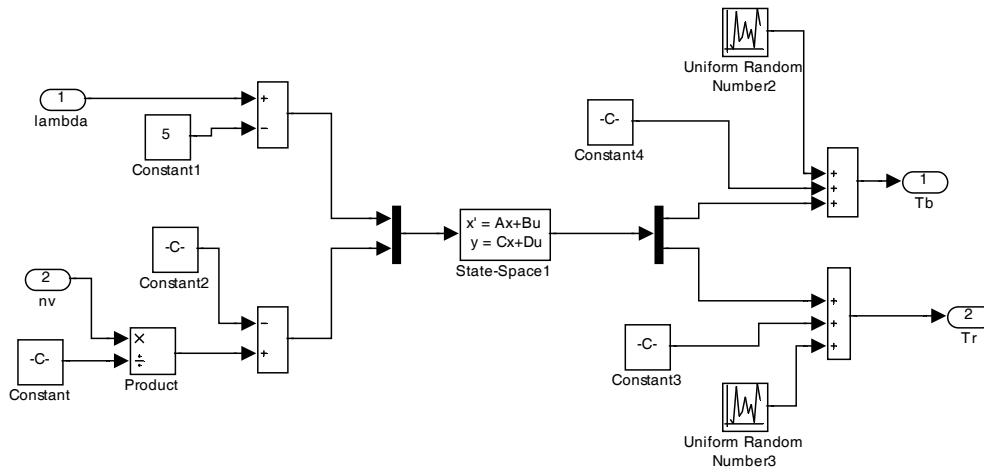


Figure 10: Linearized Simulink subsystem.

The constant blocks subtracted from the inputs are there because the state space model requires the inputs as deviation variables and the controllers will be feeding the inputs in as the actual values. The constant block divided by the n_v input is there to convert SLPM to moles/sec which is the form the state space model requires. The constant blocks added into the output temperatures are to convert the deviation variables coming from the state space model back to the actual temperatures. The uniform random number blocks generate “process noise” so the system more closely resembles an actual process.

Section 3: Model Development

Before one can begin to control a system it is necessary to have a model of the system from which a controller can be designed. The standard practice is to perform step tests to show the system’s dynamic response to an input change. A step of 10% of the input’s steady state value is usually chosen for the test because it is large enough that the response is visible over the process noise but not so large that it is uneconomical. From the responses it is a relatively simple task to determine the model parameters.

First a step of 0.5 was made in the excess air ratio, which has a steady state value of 5. This change led to a lead-lag response in the burner temperature and a first order response in the reformer temperature. The parameters from the reformer output were determined from the graph using the 63.2% method. The parameters for the burner output were more difficult to determine. In *Process Control Modeling, Design, and Simulation* (Bequette, 2003) there is a graph relating the various τ_n/τ_p ratios and from this graph it looked as if the τ_n/τ_p ratio was between one and two. Through a series of iterations the τ_n and τ_p values were determined. Sample calculations for the process parameters are given in Appendix 1.3.

Then a step change of 0.65856 SLPM was made to the methane flow rate to the burner, which has a steady state value of 6.5856 SLPM. This step change resulted in

another lead-lag response in the burner temperature and a first order response in the reformer temperature. Parameters for the models were developed in the same fashion described above.

The transfer function matrix is shown below where input one (u1) is the excess air ratio, input two (u2) is the methane flow rate to the burner in SLPM, output one (y1) is the burner temperature in deg C, and output two (y2) is the reformer temperature in deg C.

$$\begin{bmatrix} -28.548^{\circ}\text{C} \frac{500 \text{ sec}(s)+1}{400 \text{ sec}(s)} & -19.39^{\circ}\text{C} \frac{520 \text{ sec}(s)+1}{400 \text{ sec}(s)+1} \\ \frac{-45.506^{\circ}\text{C}}{730 \text{ sec}(s)+1} & \frac{-35.69^{\circ}\text{C}}{710 \text{ sec}(s)+1} \end{bmatrix} \begin{bmatrix} u_1 \\ u_2 \end{bmatrix} = \begin{bmatrix} y_1 \\ y_2 \end{bmatrix} \quad [15]$$

The process response and model responses to the input changes are shown in Figure 11 and 12. Appendix I shows the Simulink diagrams for performing the step change and developing the model.

Burner and reformer temperature responses to step change in excess air ratio

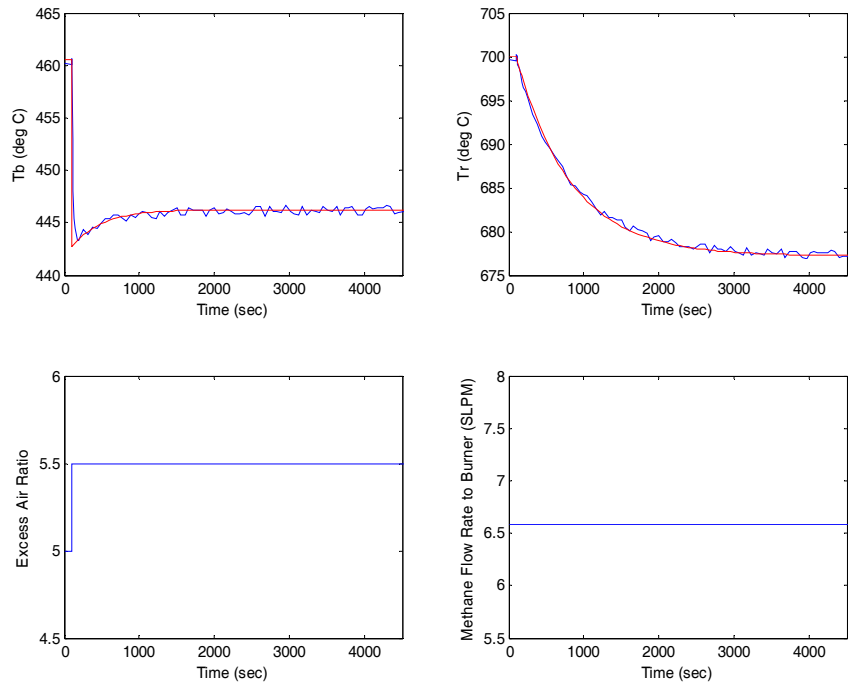


Figure 11: Process and model response to a step change in the excess air ratio.

Burner and reformer responses to step change in the methane flow rate

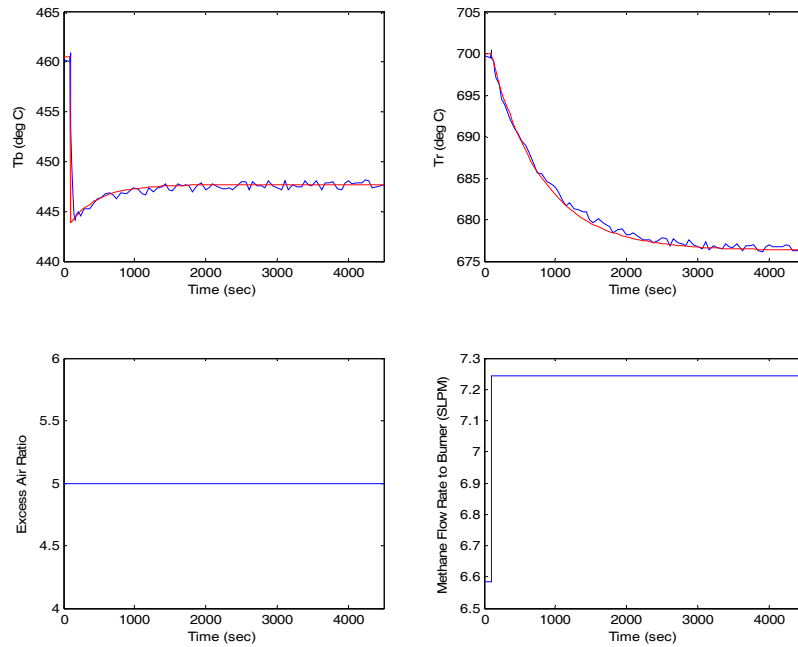


Figure 12: Model and process response to step change in the methane flow rate.

Section 4: Single Input-Single Output Controller Development

The SISO controllers were determined using IMC-based PID control because this type of control is a function of only one parameter, λ , which can be adjusted to allow for the desired response speed and robustness. This λ value should not be confused with the λ described before which is the excess air ratio. The parameters for the reformer temperature controller were designed with improved disturbance rejection. This results in a PI controller with the first order parameters given below.

$$k_c = \frac{2\tau_p - \lambda}{k_p \lambda} \quad \tau_i = \frac{2\tau_p \lambda - \lambda^2}{\tau_p} \quad [16]$$

For setpoint tracking of a lead-lag process the controller is in the PI form with a filter. The parameters are given below.

$$k_c = \frac{\tau_p}{k_p \lambda} \quad \tau_i = \tau_p \quad \tau_F = \tau_n \quad [17]$$

Sample calculations for both types of parameters are given in Appendix 1.4. A representative Simulink diagram for determining SISO control is shown in Appendix II.

By adjusting the values of λ the amount of overshoot and speed of response the process experiences can be altered. Figure 13 shows the varying burner temperature outputs when controlled by the excess air ratio. A quick response with no overshoot occurs when λ is 100 sec. The uncontrolled loop, the reformer temperature, also increases and approaches a steady state value of about 760 deg C. Figure 14 shows the different burner temperature responses when the methane flow rate controls. Again a good response is seen when λ is 100 sec and the reformer temperature once again increases but this time to a value of about 770 deg C. Figure 15 shows the reformer temperature controlled by the excess air ratio. When λ is 600 sec a quick response is seen in the reformer temperature. There is an acceptable spike down to about 3 in the excess air ratio and up to about 525 deg C the burner temperature before both converge to steady state values of approximately 3.5 and 510 deg C respectively. Figure 16 shows the reformer temperature controlled by the methane flow rate. Again good response is exhibited when λ is 600 sec with a methane flow rate spike down to 4 SLPM before returning to 4.5 SLPM and a burner temperature spike to about 520 deg C before reaching a steady state value of about 510 deg C.

Burner temperature control using the excess air ratio and varying λ

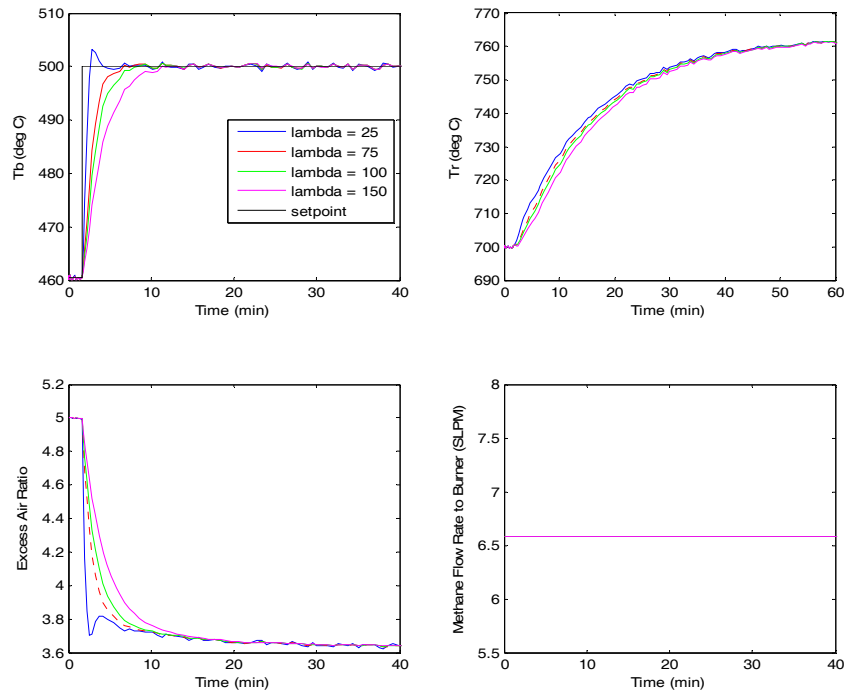


Figure 13: Burner temperature controlled by the excess air ratio. Best response when λ is 100 sec.

Burner temperature control by the methane flow rate and varying λ

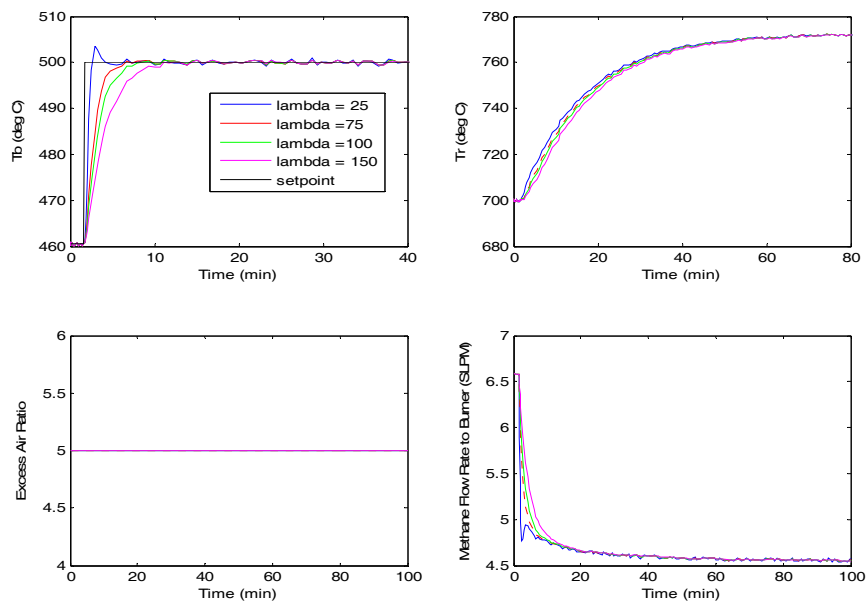


Figure 14: The burner temperature response when controlled by the methane flow rate. The best response occurs when λ is 100 sec.

Reformer temperature control by the excess air ratio and varying λ

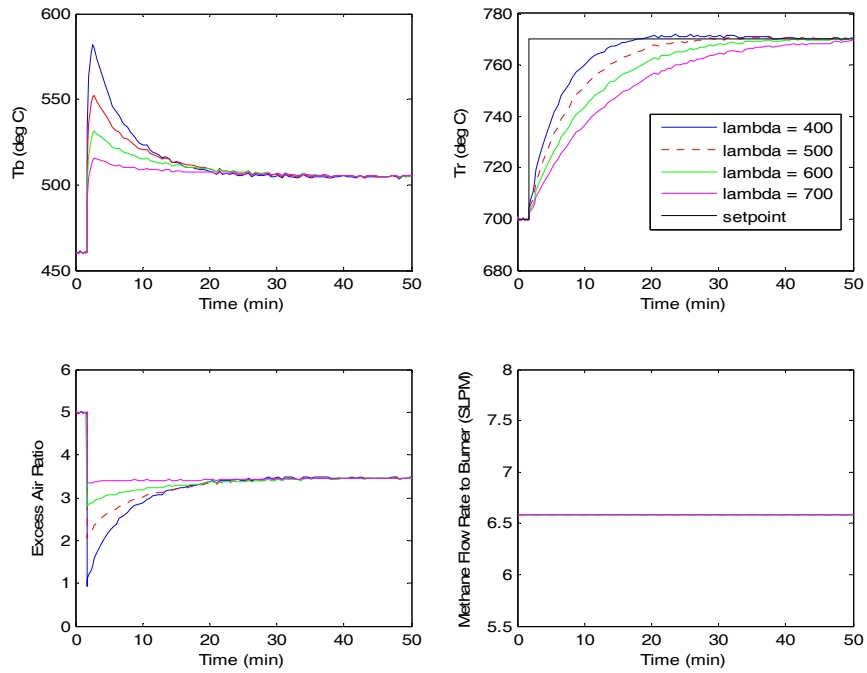


Figure 15: Reformer temperature controlled by the excess air ratio, best response when λ is 600 sec.

Reformer temperature controlled by the methane flow rate and varying λ

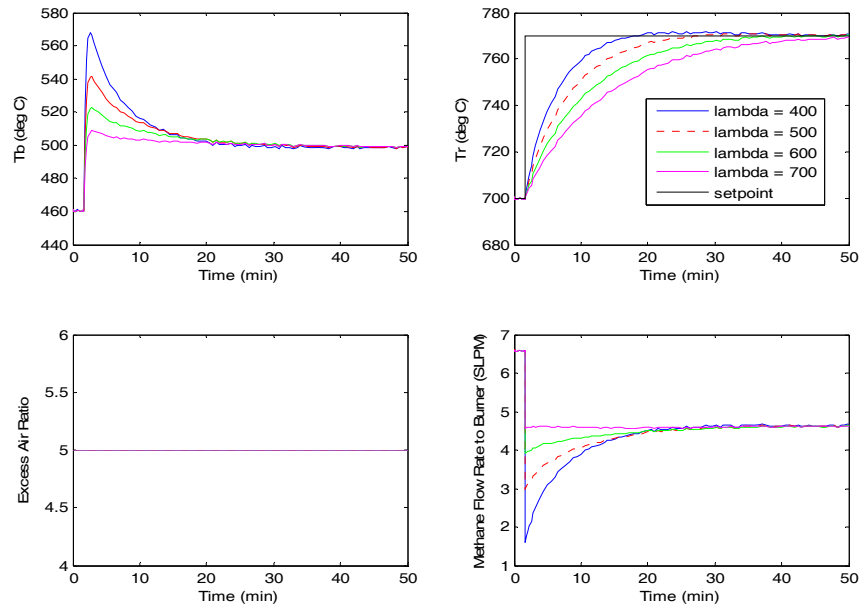


Figure 16: Reformer temperature controlled by the methane flow rate, best response λ is 600 sec.

With these λ values the controllers are as follows, where g_{c11} is the burner temperature controlled by the excess air ratio, g_{c12} where the burner temperature is controlled by the methane flow rate, g_{c21} where the reformer temperature is controlled by the excess air ratio, and g_{c22} where the reformer temperature is controlled by the methane flow rate:

$$\begin{aligned} g_{c11} &= -0.1401 \left(1 + \frac{1}{400s}\right) \left(\frac{1}{500s+1}\right) & g_{c12} &= -0.2063 \left(1 + \frac{1}{400s}\right) \left(\frac{1}{520s+1}\right) \\ g_{c21} &= -0.0315 \left(1 + \frac{1}{706.85s}\right) & g_{c22} &= -0.0383 \left(1 + \frac{1}{692.96s}\right) \end{aligned} \quad [18]$$

Section 5: Multivariable Control Loops

Single input-single output control determines stability when one loop is open so the next step is to design controllers that can maintain stability when both loops are closed. To determine which input to pair with which output a relative gain analysis is used. The gain matrix, the process gains associated with each SISO loop, is given below.

$$K = \begin{bmatrix} -28.548 & -19.39 \\ -45.506 & -35.69 \end{bmatrix} \quad [19]$$

Sample calculations for determining the values in the relative gain array are given in Appendix 1.5. The relative gain array is given below.

$$\Lambda = \begin{bmatrix} 7.463 & -6.463 \\ -6.463 & 7.463 \end{bmatrix} \quad [20]$$

The best pairing occurs on the y1-u1 (burner temperature and excess air ratio) and y2-u2 (reformer temperature and methane flow rate) inputs and outputs. It is preferable to pair when a system has relative gains close to one so that the gain the process exhibits when both loops are closed is not significantly different from gain experienced when one of the loops is open but in this system the relative gains are not close to one. The system cannot be paired on a negative relative gain because it would mean that the process and the controller gains will have different signs.

Based on the RGA analysis there is no need to detune the λ values found when performing SISO control. With a relative gain greater than one the multivariable loop's lambda values should be found when the other loop is closed which is in essence SISO control.

When pairing the excess air ratio with the burner temperature the λ value is 100 sec and when pairing the methane flow rate with the reformer temperature the λ value is 600 sec. When both loops are closed and these λ values are used a good response to setpoint changes can be seen. This is demonstrated in Figure 17 below. The Simulink diagram when both loops are closed is shown in Appendix III.

MV y1-u1 and y2-u2 pairing

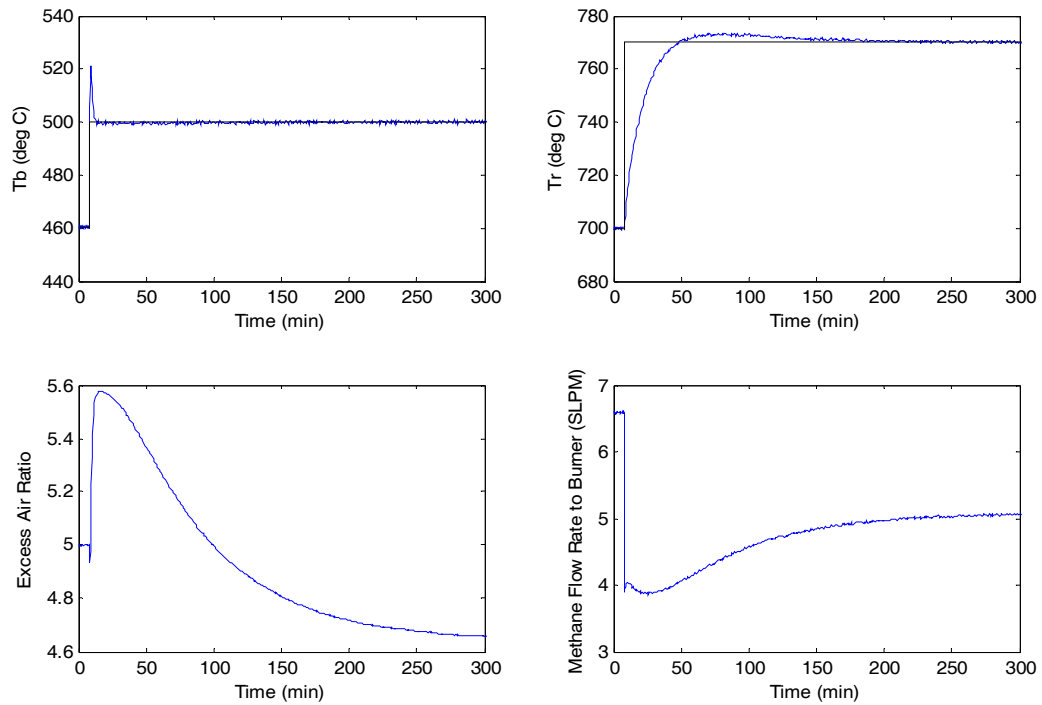


Figure 17: System response when the burner temperature is changed to 500 deg C and the reformer temperature is changed to 770 deg C. The burner temperature spikes to 520 deg C but reaches setpoint more quickly than the reformer. The excess air ratio and methane flow rates remain physically possible (i.e.: no negative flow rates).

Setpoint changes can be made in only one of the outputs and the system should continue to exhibit a good response. Figures 18 and 19 illustrate this situation.

MV burner temperature setpoint change

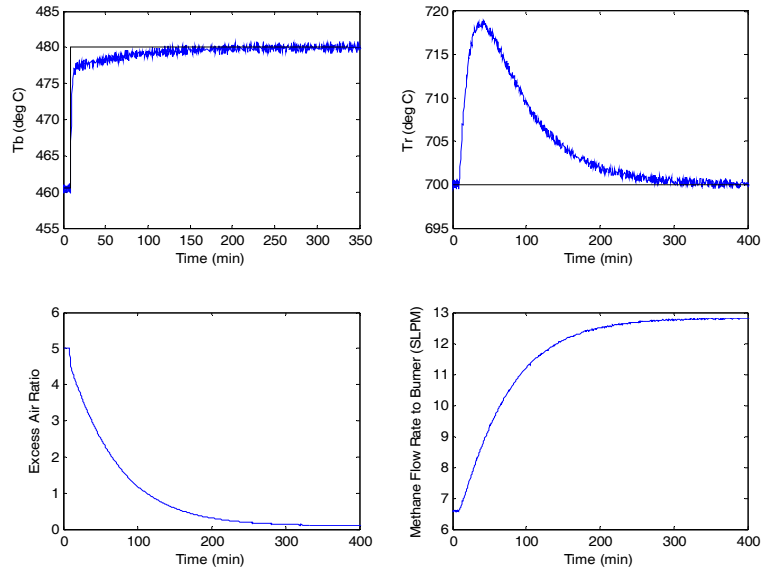


Figure 18: The burner temperature was changed to 480 deg C. The reformer temperature increases to about 720 deg C and the methane flow rate almost reaches 13 SLPM but both remain within their operating range. The excess air ratio is approaching zero and so a stepchange in the burner temperature greater than 20 deg C is probably not possible with only one loop closed.

MV reformer temperature setpoint change

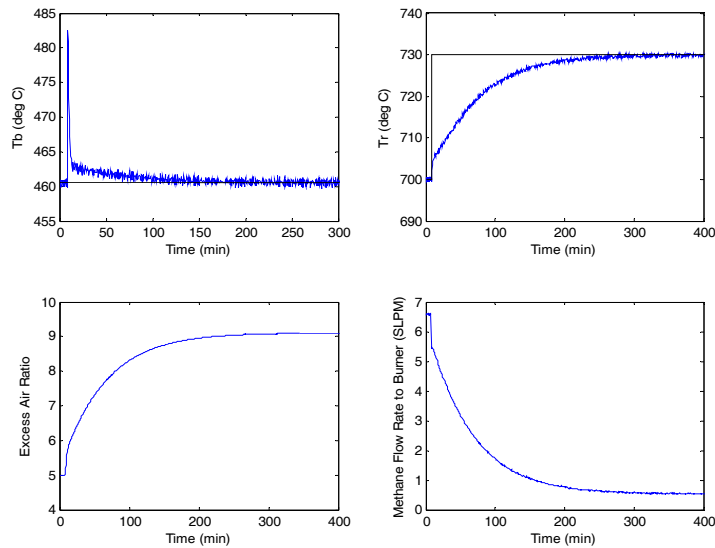


Figure 19: Reformer temperature step to 730 deg C. The burner temperature spikes to about 483 deg C when the step is made but the temperature is within operating parameters. The methane flow rate is approaching zero and so a step change greater than 30 deg C in the reformer temperature is probably not physically possible with one loop open.

One final thing to consider is the importance of maintaining control if one of the loops were to fail open or be put on manual mode. This situation is exactly the same as that presented when performing SISO control and since the λ values have not been adjusted the system should remain stable. Figures 20 and 21 show the process's response when a step change is made in either temperature while the other loop is open.

Output responses with the methane flow rate loop open

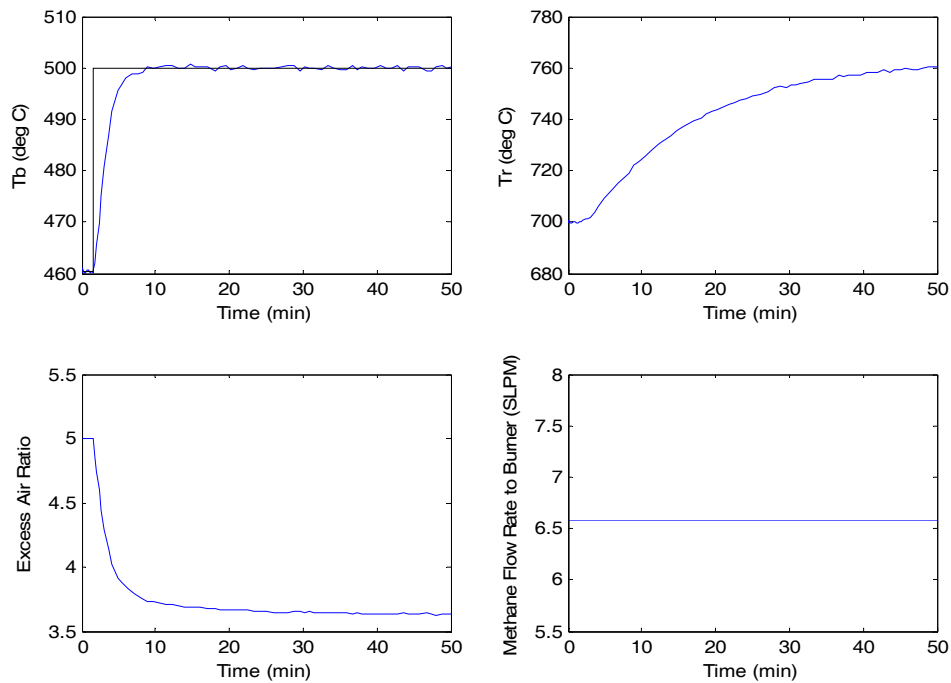


Figure 20: Burner setpoint can be reached when the methane flow rate loop is open.

Output Responses with the excess air ratio loop open

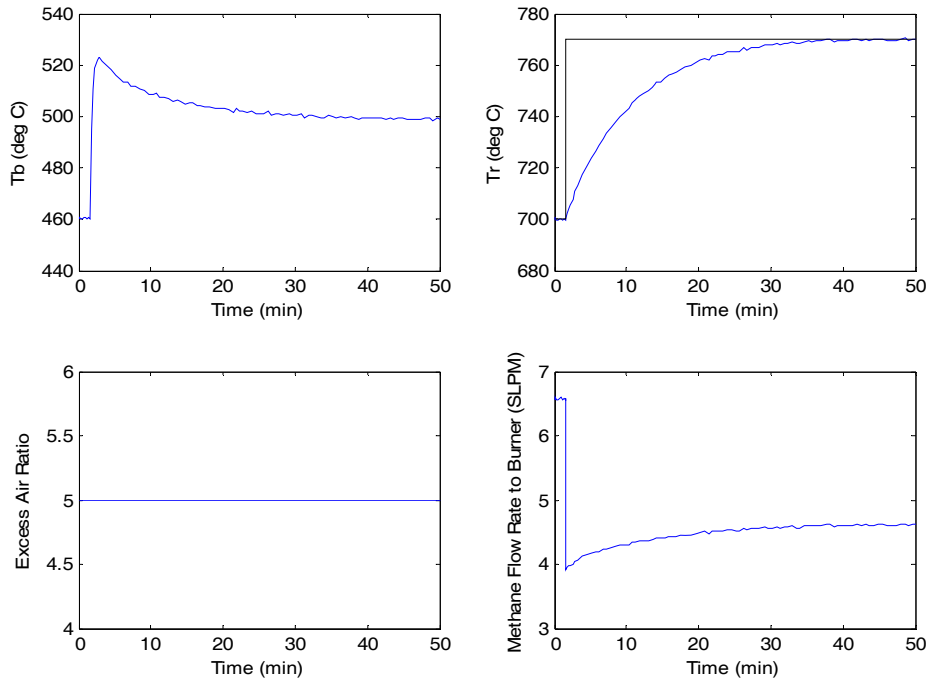


Figure 21: Reformer setpoint can be reached with the excess air ratio loop open.

Section 6: Disturbance Rejection

Good rejection of disturbances is an important aspect of control. The reformer controller was designed with disturbance rejection but the burner controller was not because all the disturbances that would be seen in the system would occur in the reformer catalyst. When a disturbance, such as catalyst sintering occurs, it is necessary to be able to quickly return the temperatures to setpoint. Figure 22 shows the difference in response between a regular reformer controller and one designed with improved disturbance rejection when 100% sintering occurs. There is no difference in the response in the burner temperature but the recovery of the reformer temperature is slightly faster when controlled by a system designed to reject disturbances. The controller design parameters for a first order system without disturbance rejection are given below. The Simulink diagram for disturbances is shown in Appendix IV.

$$k_c = \frac{\tau_p}{k_p \lambda} \quad \tau_l = \tau_p \quad [7]$$

MV rejection of sintering disturbance

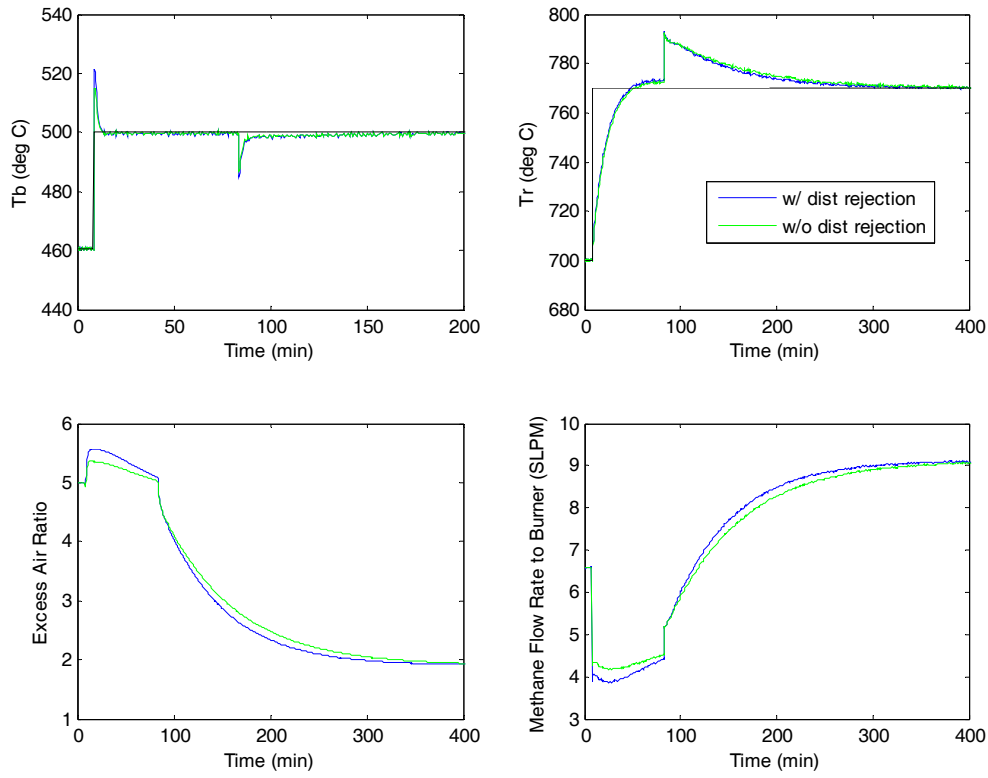


Figure 22: Response of the system to a disturbance rejection. With a controller designed for improved disturbance rejection there is a slight decrease in time required to return to reformer temperature setpoint.

Section 7: Scaling, SVD, and Directional Sensitivity

In multivariable control it is often easier to make changes in certain directions. Singular value decomposition can be used to determine the simplest and most difficult directions in which changes can be made, called directional sensitivity. First the gain matrix must be scaled to have maximum and minimum changes of one. The scaling matrices for the inputs and outputs are determined by the maximum and minimum values of the inputs and outputs. In this report the nominal values of both the inputs and the outputs represented fell in the middle of the range of inputs and outputs. The maximum input values were twice the nominal values, the maximum burner temperature was 200 deg C greater than the nominal value, and the maximum reformer temperature was 950 deg C which represents the temperature at which heat damage could be experienced by the system. The method for determining these scaling matrices is given in Appendix 1.7. Below are the output (S_O) and input (S_I) scaling matrices.

$$S_o = \begin{bmatrix} \frac{1}{200} & 0 \\ 0 & \frac{1}{249.997} \end{bmatrix} \quad S_I = \begin{bmatrix} \frac{1}{5} & 0 \\ 0 & \frac{1}{6.5846} \end{bmatrix} \quad [21]$$

The scaled gain matrix, G^* , is given below, where G is the process gain matrix:

$$G^* = S_o \times G \times S_I^{-1} \quad [22]$$

The Matlab code for determining G^* is given in Appendix 1.7. G^* is given below:

$$G^* = \begin{bmatrix} -0.7137 & -0.6385 \\ -0.9101 & -0.9402 \end{bmatrix} \quad [23]$$

This scaled gain matrix can be used in SVD analysis to determine the strongest and weakest output and input directions.

$$G^* = U \Sigma V^T \quad [24]$$

U is a matrix in which the first column represents the strongest output direction and the second column represents the weakest output direction. Σ is a matrix where the ratio of the numbers on the diagonal represent how well conditioned the system is. For example if the ratio of the minimum to maximum values is large then the system is ill-conditioned. V is a matrix in which the first column represents the strongest input direction and the second column indicates the weakest input direction. The Matlab code used to determine the SVD matrices is given in Appendix 1.6. The SVD matrices are shown below:

$$\begin{bmatrix} -0.7137 & -0.6385 \\ -0.9101 & -0.9402 \end{bmatrix} = \begin{bmatrix} -0.5903 & -0.8072 \\ -0.8072 & 0.5903 \end{bmatrix} \begin{bmatrix} 1.6206 & 0 \\ 0 & 0.0555 \end{bmatrix} \begin{bmatrix} 0.7133 & 0.7009 \\ 0.7009 & -0.7133 \end{bmatrix}^T \quad [25]$$

To scale the matrices back to the actual process is a simple process shown in Appendix 1.7. The easiest output direction changes are given in equation 26. The most difficult output changes to make are given in equation 27.

$$\begin{bmatrix} y_1 \\ y_2 \end{bmatrix} = \begin{bmatrix} -118.06 \\ -201.7976 \end{bmatrix} \quad [26]$$

$$\begin{bmatrix} y_1 \\ y_2 \end{bmatrix} = \begin{bmatrix} -161.44 \\ 147.5732 \end{bmatrix} \quad [27]$$

The results of mapping the input changes to the output changes in the strong and weak directions are shown in Figure 23.

SVD Input to Output Mapping

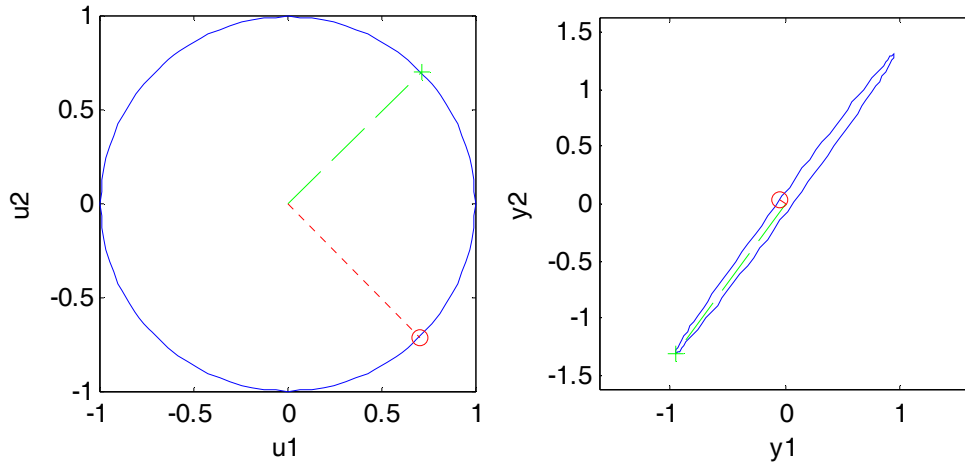


Figure 23: The circle shows the scaled directions in which changes can be made in the inputs. The ellipse shows the scaled output directions in which the process can move. The green line represents the strongest direction and the red line represents the weakest direction.

The process response to setpoint changes in the strongest and weakest directions are shown in Figures 24 and 25. A change of ten percent of the total possible magnitude of change was used in developing these responses because a step increase should be as small as possible. In the strongest direction response there is a very small initial spike in the burner temperature and a minimum amount of change in both the excess air ratio and the methane flow rate. When the weakest direction is applied not only is there an inverse response in the reformer temperature, but the process requires a negative methane flow rate that is not physically possible.

Setpoint changes in the strong direction

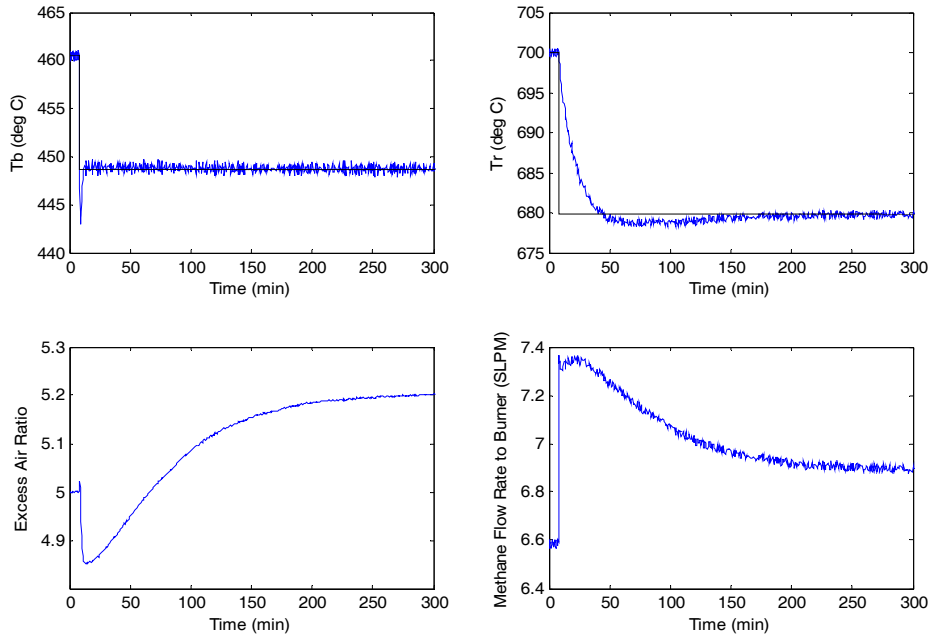


Figure 24: A burner temperature change of -11.806 deg C and a reformer temperature change of -20.17976 are the easiest to implement.

Setpoint changes in the weakest direction

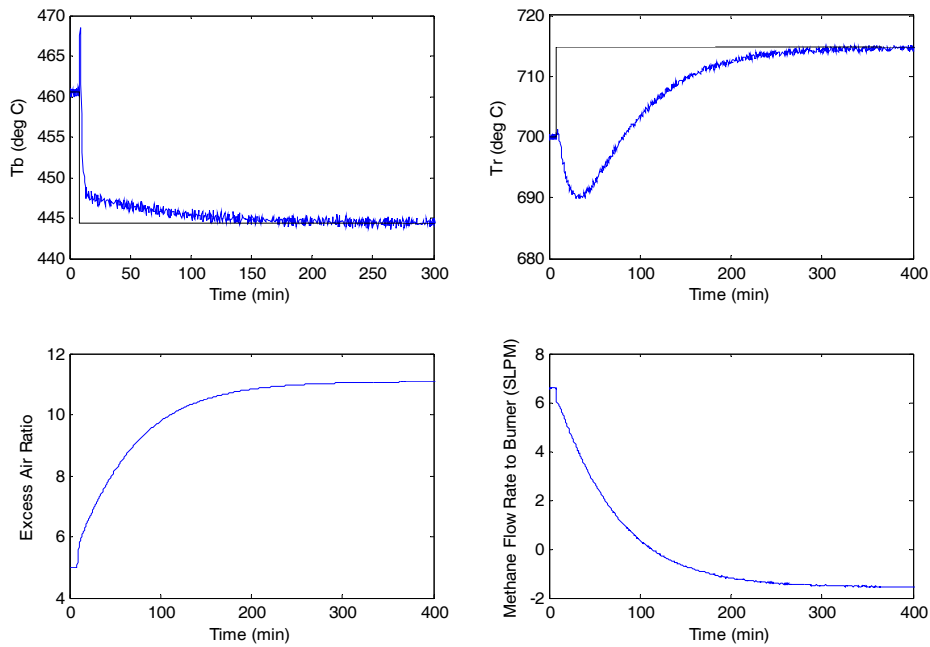


Figure 25: A burner temperature change of -16.144 deg C and a reformer temperature increase of 14.75732 are the hardest setpoint changes to make. In fact, it causes the methane flow rate to become negative.

Section 8: Recommendations

Fuel cell reformers are difficult to control and can be quite challenging. The limited range of setpoint changes that can be made make it especially difficult to maintain a physically possible system. Reset windup could easily occur if a setpoint change was made that required input rates beyond the physical capabilities of the system. An anti-reset windup strategy could be implemented to account for this problem.

The type of disturbance modeled in this report was that of catalyst sintering. A step change does not really accurately model this problem because sintering is a disturbance that occurs over time and not at one instant. Also, this system does not take into account the impulse disturbance of catalyst hotspots that could occur.

Finally, a more general issue is that this is a linearized model of a non-linear system. If the model outputs were compared to the actual outputs of a real system the temperature and flow rates might not be equal. This means that this control strategy could be ineffective when trying to control an actual reformer and some type of non-linear system control would need to be developed.

References:

- Bequette, B. Wayne. *Process Control Modeling, Design, and Simulation*. New Jersey, 2003, p 110.
- Dicks, A.L., “Advances in catalysts for internal reforming in high temperature fuel cells,” *Journal of Power Sources*, v 71, n 1-2, 1998, p 111-122.
- Jahn, H., Schroer, W., “Dynamic simulation model of a steam reformer for a residential fuel cell power plant,” *Journal of Power Sources*, v 150, n 1-2, 2005, p 101-109.
- Larminie, James and Andrew Dicks. *Fuel Cell Systems Explained*. John Wiley and Sons Ltd., ed 2, 2003.
- Meshcheryakov, V. D., Kirillov, V. A., Sobyenin, V.A., “Thermodynamic analysis of a solid oxide fuel cell power system with external natural gas reforming,” *Theoretical Foundations of Chemical Engineering*, v 40, n 1, 2006, p 51-58.
- Pukrushpan, J.T., Stefanopoulou, A.G., Varigonda, S. et al, “Control of natural gas catalytic partial oxidation for hydrogen generation in fuel cell applications,” *IEEE Transactions on Control Systems Technology*, v 13, n 1, Jan. 2005, p 3-14.
- Radulescu, M., Lottin, O., et al, “Experimental and theoretical analysis of the operation of a natural gas cogeneration system using a polymer exchange membrane fuel cell,” *Chemical Engineering Science*, v 61, n 2, 2006, p 743-752.

Appendices

Appendix 1.2

Matlab file for simultaneously solving the system of differential equations. This file only needs to exist and saved as 'outcomp', no modifications are made to this one.

```
function xdot = outcomp(t,x,flag,sc,nCH4i,lambda)
```

```
%states%
```

```
Tw = x(1);
```

```
Tg = x(2);
```

```
Tb = x(3);
```

```
Te = x(4);
```

```
Tr = x(5);
```

```
%heat capacities J/K
```

```
Cw = 7.27e3;
```

```
Cb = .22e3;
```

```
Ce = 5.42e3;
```

```
Cg = 2.44e3;
```

```
Cr = 3.61e3;
```

```
%heat exchange coefficients W/K
```

```
kbr = 1.32e-9;
```

```
kgb = 4.5;
```

```
kgw = 5.16;
```

```
kea = .439;
```

```
kre = 16.3;
```

```
kwa = 1.16;
```

```
kfb = 16.1;
```

```
kfg = .3;
```

```
%heat capacity coefficients
```

```
Rgas = 8.314; % Gas constant, units of J/mol-K
```

```
A_o2 = 3.639;
```

```
B_o2 = 0.506e-3;
```

```
C_o2 = 0;
```

```
D_o2 = -0.227e5;
```

```
A_n2 = 3.280;
```

```
B_n2 = 0.593e-3;
```

```
C_n2 = 0;
```

```
D_n2 = 0.040e5;
```

```
A_ch4 = 1.702;
```

```
B_ch4 = 9.081e-3;
```

```
C_ch4 = -2.164e-6;
```

```
D_ch4 = 0;
```

```
A_co2 = 5.457;
```

```
B_co2 = 1.045e-3;
```

```
C_co2 = 0;
```

```
D_co2 = -1.157e5;
```

```
A_h2o = 3.470;
```

```
B_h2o = 1.450e-3;
```

```
C_h2o = 0;
D_h2o = 0.121e5;
A_h2o_L = 8.712;
B_h2o_L = 1.25e-3;
C_h2o_L = -0.18e-6;
D_h2o_L = 0;
```

%temperatures

```
Ta = 298; %ambient air temp
TH2O = 298; %temp of inlet water
TCH4 = 298; %temp inlet methane
```

%enthalpy changes

```
deltah0 = 206000; %J/mol
deltah1 = -41000; %J/mol
deltahc = -804000; %J/mol
```

%heat of evaporation H2O J/kg

```
r = -285830;
```

%initial flow rates mol/s

```
nCH4i = (nCH4i/60)*(1/22.4); %convert SLP to molar flow rate
nH2Oi = sc*nCH4i; %initial steam flow rate
```

%calculate delta n

```
po = ([195 88.22 -5.504 -9.538 -30.41 7.821 -2.223 -27.16 -4.443 7.684])*(1e-3);
p1 = ([134.5 14.02 -19.62 2.491 -11.94 .09909 .3631 .7817 2.711 -2.11])*(1e-3);
alpha = (Tr/100)-9;
beta = sc-3.5;
u = [1 alpha alpha^2 alpha^3 beta beta^2 beta^3 alpha*beta (alpha^2)*beta alpha*(beta^2)];
deltan0 = po*u*nH2Oi;
deltan1 = p1*u*nH2Oi;
```

%calculate molar flow rate to burner & reformer (mol/s)

```
v0 = -2.46e-4; %mol/s
v1 = 4.1e-3; % molV/s
sv = 1.25; %burner valve position
nv = v0+v1*sv; %CH4 flow rate to burner (mol/s)
nH2O = nH2Oi-deltan0-deltan1; %H2O flow rate to reformer
nCH4 = nCH4i-deltan0; %methane flow rate to reformer
```

%burner components gas flow rate mol/s

```
nbO2 = 2*lambda*nv;
nbN2 = 2*(79/21)*lambda*nv;
nbCH4 = nv;
```

```
nb = nbO2+nbN2+nbCH4; %burner flow rate
```

```
ybO2 = nbO2/nb;
ybN2 = nbN2/nb;
ybCH4 = nbCH4/nb;
```

%burner heat capacity calculations

```
cpbo2 = Rgas*(A_o2 + B_o2*Tb + C_o2*Tb*Tb + D_o2*(Tb^2));
```

```

cpbn2 = Rgas*(A_n2 + B_n2*Tb + C_n2*Tb*Tb + D_n2*(Tb^2));
cpbch4 = Rgas*(A_ch4 + B_ch4*Tb + C_ch4*Tb*Tb + D_ch4*(Tb^2));

cpb = cpbo2*ybO2+cpbn2*ybN2+cpbch4*ybCH4; %burner heat capacity

```

```

%temp flame and flue gas
Tf = Tb-((deltahc*nbCH4)/(cpbch4*nb+kfb)); %temp of flame
Tfg = Tf - kfg*(Tf-Tg); %temp of flue gas

```

```

%flue components gas flow rate mol/s
nfO2 = 2*(lambda-1)*nv;
nfN2 = 2*(79/21)*lambda*nv;
nfCO2 = nv;
nfH2O = 2*nv;

```

```

nf = nfO2+nfN2+nfCO2+nfH2O; %flue gas flow rate

```

```

yfO2 = nfO2/nf;
yfN2 = nfN2/nf;
yfCO2 = nfCO2/nf;
yfH2O = nfH2O/nf;

```

```

%flue gas heat capacity calc
cpfo2 = Rgas*(A_o2 + B_o2*Tf + C_o2*Tf*Tf + D_o2*(Tf^2));
cpfn2 = Rgas*(A_n2 + B_n2*Tf + C_n2*Tf*Tf + D_n2*(Tf^2));
cpfco2 = Rgas*(A_co2 + B_co2*Tf + C_co2*Tf*Tf + D_co2*(Tf^2));
cpfh2o = Rgas*(A_h2o + B_h2o*Tf + C_h2o*Tf*Tf + D_h2o*(Tf^2));

cpf = cpfo2*yfO2+cpfn2*yfN2+cpfco2*yfCO2+cpfh2o*yfH2O;

```

```

% Evaporator heat capacities
cpeH2O = Rgas*(A_h2o_L + B_h2o_L*Te + C_h2o_L*Te*Te + D_h2o_L*(Te^2));
cpeCH4 = Rgas*(A_ch4 + B_ch4*Te + C_ch4*Te*Te + D_ch4*(Te^2));

```

```

% Reactor heat capacities
cprH2O = Rgas*(A_h2o + B_h2o*Tr + C_h2o*Tr*Tr + D_h2o*(Tr^2));
cprCH4 = Rgas*(A_ch4 + B_ch4*Tr + C_ch4*Tr*Tr + D_ch4*(Tr^2));

```

```

%modeling equations
dTwdt = (kgw*(Tg-Tw)-kwa*(Tw-Ta)-cpb*nb*(Tw-Ta))/Cw; %wall
dTgdt = (kgb*(Tb-Tg)-kgw*(Tg-Tw)+kfg*cpf*nf*(Tf-Tg))/Cg; %ground plate
dTbdt = (kfb*(Tf-Tb)-cpb*nb*(Tb-Tw)-kbr*(Tb^4-Tr^4)-kgb*(Tb-Tg))/Cb; %burner
dTedt = (kre*(Tr-Te)+cpf*nf*(Tr-Te)-r*nH2Oi-cpeH2O*nH2O*(Te-TH2O)-cpeCH4*nCH4*(Te-
TCH4)-kea*(Te-Ta))/Ce; %evaporator
dTrdt = (kbr*(Tb^4-Tr^4)-kre*(Tr-Te)+cpf*nf*(Tfg-Tr)-deltah0*deltan0-deltah1*deltan1-
cprH2O*nH2O*(Tr-Te)-cprCH4*nCH4*(Tr-Te))/Cr; %reactor

```

```

xdot = [dTwdt;dTgdt;dTbdt;dTedt;dTrdt];

```

In this m-file adjust the values of nCH4i (initial methane flow rate to the reformer), sc (steam to carbon ratio), and lambda (excess air ratio) as desired. Save the file under

whatever name desired and type the name into the command window to get a plot of the steady state values for the different temperatures.

```
x0 = [700;700;800;850;900]; %initial steady state value guesses
```

```
%adjustable variables
```

```
nCH4i=9.5;
```

```
sc = 3.0076;
```

```
lambda = 5;
```

```
[T,Y]=ode45(@outcomp,[0 9000],x0,[],[],sc,nCH4i,lambda);
```

```
Tw = Y(length(Y),1) - 273.15;
```

```
Tg = Y(length(Y),2) - 273.15;
```

```
Tb = Y(length(Y),3) - 273.15;
```

```
Te = Y(length(Y),4) - 273.15;
```

```
Tr = Y(length(Y),5) - 273.15;
```

```
str1='Tw = ';
```

```
str2=num2str(Tw);
```

```
str3=strcat(str1,str2);
```

```
str4='Tg = ';
```

```
str5=num2str(Tg);
```

```
str6=strcat(str4,str5);
```

```
str7='Tb = ';
```

```
str8=num2str(Tb);
```

```
str9=strcat(str7,str8);
```

```
str10='Te = ';
```

```
str11=num2str(Te);
```

```
str12=strcat(str10,str11);
```

```
str13='Tr = ';
```

```
str14=num2str(Tr);
```

```
str15=strcat(str13,str14);
```

```
plot(Y)
```

```
xlabel('time (sec)')
```

```
ylabel('Temperature (K)')
```

```
legend('Tw','Tg','Tb','Te','Tr')
```

```
text(600,600,str3)
```

```
text(600,640,str6)
```

```
text(600,680,str9)
```

```
text(600,710,str12)
```

```
text(600,750,str15)
```

Appendix 1.3

Calculations to determine the model parameters for the processes.

g_{p11} : burner temperature response to change in excess air ratio

$$k_p = \frac{\Delta y}{\Delta u} = \frac{460.524 - 446.25}{5 - 5.5} = -28.548^\circ C$$

g_{p12} : burner temperature response to change in methane flow rate

$$k_p = \frac{460.524 - 447.75}{6.5856 - 7.24416} = -19.39^\circ C$$

g_{p21} : reformer temperature response to change in excess air ratio

$$k_p = \frac{700.003 - 677.35}{5 - 5.5} = -45.506^\circ C$$

$$\tau_p = .632(677.25 - 700.003) = -14.38 + 700.003 = 685.623^\circ C \text{ occurs at } 830 \text{ sec}$$

$$\tau_p = 830 - 100 = 730 \text{ sec}$$

g_{p21} : reformer temperature response to change in methane flow rate

$$k_p = \frac{700.003 - 676.5}{6.5856 - 7.24416} = -35.69^\circ C$$

$$\tau_p = .632(676.5 - 700.003) = -14.85 + 700.003 = 685.15^\circ C \text{ occurs at } 810 \text{ sec}$$

$$\tau_p = 810 - 100 = 710 \text{ sec}$$

Appendix 1.4

Sample calculation to determine the tuning parameters for the first order response g_{c21} .

$$k_c = \frac{2\tau_p - \lambda}{k_p \lambda} = \frac{2(730) - \lambda}{-45.506\lambda} \quad \tau_I = \frac{2\tau_p \lambda - \lambda^2}{\tau_p} = \frac{2(730)\lambda - \lambda^2}{730}$$

Sample calculation to determine the tuning parameters for the lead-lag response g_{c12} .

$$k_c = \frac{\tau_p}{k_p \lambda} = \frac{400}{-28.7\lambda} \quad \tau_I = \tau_p = 400 \quad \tau_F = \tau_N = 500$$

Appendix 1.5

Equations to determine the relative gain array.

$$\Lambda = \begin{bmatrix} \frac{k_{11}k_{22}}{k_{11}k_{22} - k_{12}k_{21}} & \frac{-k_{12}k_{21}}{k_{11}k_{22} - k_{12}k_{21}} \\ \frac{-k_{21}k_{12}}{k_{11}k_{22} - k_{12}k_{21}} & \frac{k_{11}k_{22}}{k_{11}k_{22} - k_{12}k_{21}} \end{bmatrix} = \begin{bmatrix} \lambda_{11} & \lambda_{12} \\ \lambda_{21} & \lambda_{22} \end{bmatrix}$$

$$\lambda_{11} = \frac{(-28.548)(-35.69)}{(-28.548)(-35.69) - (-19.39)(-45.506)} = 7.463$$

Appendix 1.7

Table to determine the range associated with each input and output:

	Min Value	Nominal Value	Max Value	½ Range
y 1 (burner)	260.524	460.524	660.524	200
y 2 (reformer)	450.006	700.003	950	249.997
u 1 (excess air)	0	5	10	5
u 2 (methane)	0	6.5846	13.1712	6.5846

From this table the output and input scaling matrices were developed:

$$S_o = \begin{bmatrix} \frac{1}{\frac{1}{2}range(y1)} & 0 \\ 0 & \frac{1}{\frac{1}{2}range(y2)} \end{bmatrix} = \begin{bmatrix} \frac{1}{200} & 0 \\ 0 & \frac{1}{249.997} \end{bmatrix}$$

$$S_i = \begin{bmatrix} \frac{1}{\frac{1}{2}range(u1)} & 0 \\ 0 & \frac{1}{\frac{1}{2}range(u2)} \end{bmatrix} = \begin{bmatrix} \frac{1}{5} & 0 \\ 0 & \frac{1}{6.5846} \end{bmatrix}$$

The Matlab code for determining the G^* matrix is given below:

```
>> So=[1/200 0; 0 1/249.997]
```

So =

```
0.0050    0
    0 0.0040
```

```
>> Si=[1/5 0; 0 1/6.5856]
```

Si =

```
0.2000    0
    0 0.1518
```

```
>> invSi=inv(Si)
```

invSi =

```
5.0000    0
    0 6.5856
```

```
>> G=[-28.548 -19.39; -45.506 -35.69]
```

G =

```
-28.5480 -19.3900
-45.5060 -35.6900
```

```
>> Gstar=So*G*invSi
```

Gstar =

```
-0.7137 -0.6385
-0.9101 -0.9402
```

Matlab code to determine the SVD matrices:

```
>> [U,S,V]=svd(Gstar)
```

U =

```
-0.5903 -0.8072
-0.8072  0.5903
```

S =

$$\begin{bmatrix} 1.6206 & 0 \\ 0 & 0.0555 \end{bmatrix}$$

V =

$$\begin{bmatrix} 0.7133 & 0.7009 \\ 0.7009 & -0.7133 \end{bmatrix}$$

To scale the easy direction back to the actual process:

$$y = S_0^{-1} \times y^*$$

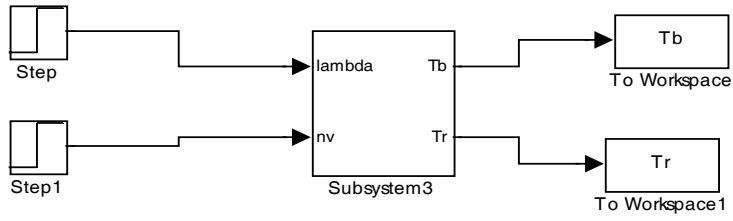
Where y^* is a matrix of the strong directions for the outputs.

$$y = \begin{bmatrix} 200 & 0 \\ 0 & 249.997 \end{bmatrix} \begin{bmatrix} -0.5903 \\ -0.8072 \end{bmatrix} = \begin{bmatrix} -118.06 \\ -201.7976 \end{bmatrix}$$

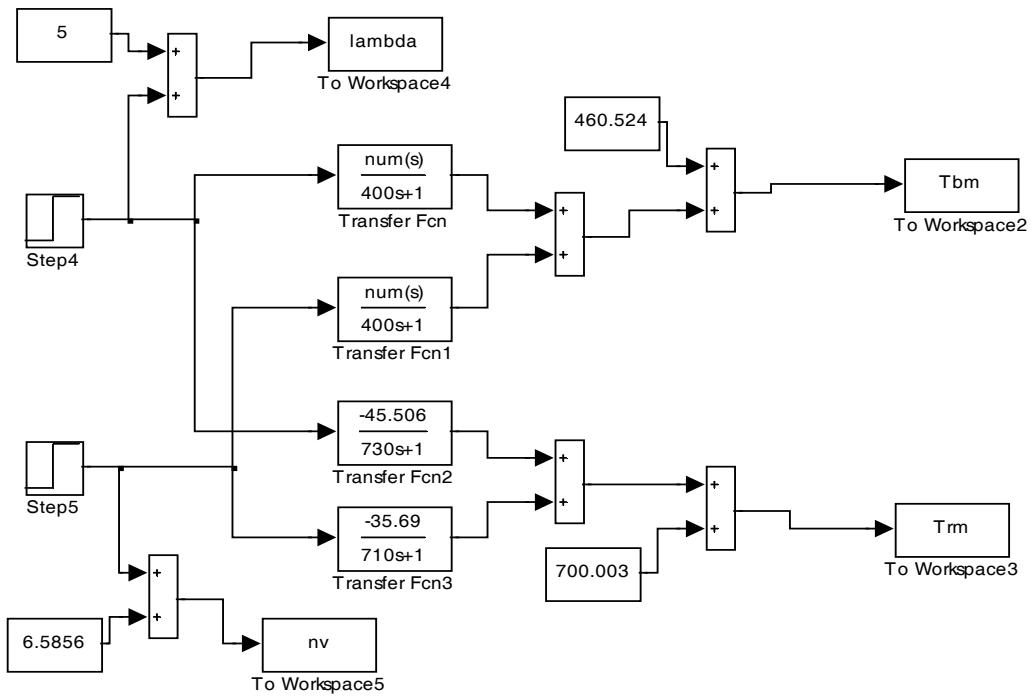
Ten percent of these outputs result in a temperature decrease of 11.806 deg C and a reformer decrease of 20.1798 deg C. The same process is used to determine the weakest output direction and the strongest and weakest direction of the inputs.

Appendix I:

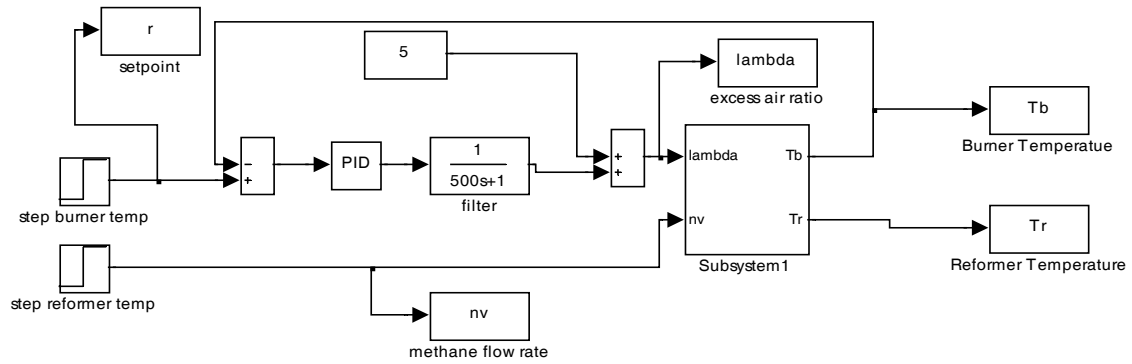
Process Diagram



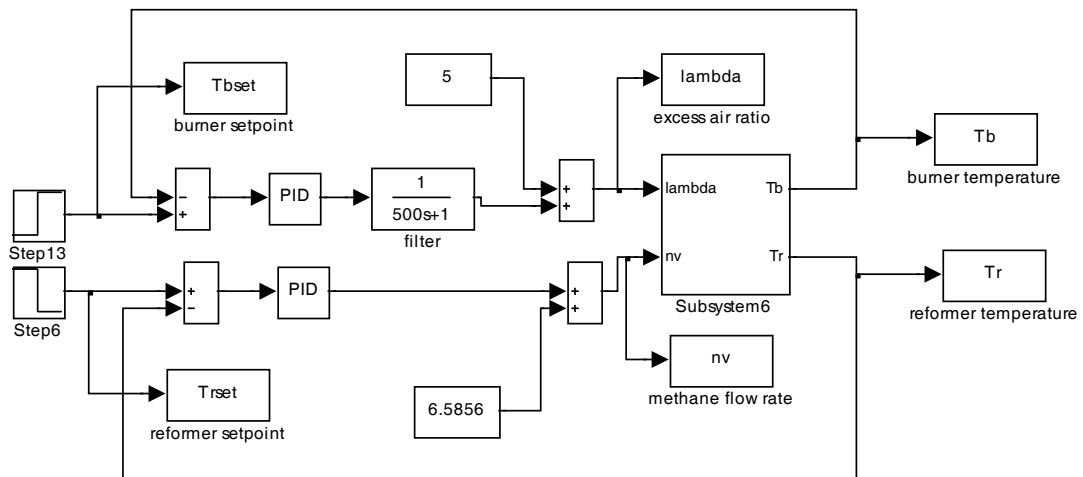
Model Diagram



Appendix II:



Appendix III:



Appendix IV:

